CERN - EUROPEAN ORGANIZATION FOR NUCLEAR RESEARCH

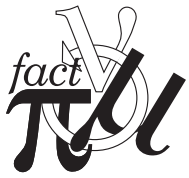

NuFact Note 2000-78
September 6, 2001

Study of (anti-)Neutrino Fluxes from a Horn Neutrino Beam using 2.2 GeV protons

A. Blondel[a], M. Donegà[b1], S. Gilardoni [a2]

[a] Département de Physique, Université de Genève, Switzerland
[b] Dipartimento di fisica, Universitá degli studi di Milano

Abstract

This note presents improved calculations of the neutrino flux for a conventional, horn focused, (anti-)neutrino beam from CERN SPL. The effect of muon polarization is included. The sensitivity of the flux and of the electron-neutrino contamination upon decay tunnel length and width is presented.

[1]CERN and Erasmus student at the Université de Genève
[2]Supported by the CERN Doctoral Student Program.

1 Introduction

A first evaluation of neutrino fluxes obtainable with CERN SPL and a conventional horn-focused beam was proposed in reference [1]. Based on the same horn study [2], [3], neutrino fluxes are calculated by considering the pion decay and subsequent muon decay, taking into account muon polarization. The sensitivity of the fluxes upon decay tunnel parameters is investigated. The aim is to enhance the performance of the system for the search of $\nu_\mu \rightarrow \nu_e$ oscillations, for which the intrinsic ν_e component of the beam constitutes an irreducible background.

2 System configuration

The configuration is the same as used in reference [1]. Pions are produced from a proton beam of 2.2 GeV (kinetic energy) impinging on a liquid Hg target and focused with a magnetic horn (Figure 1). The horn geometry was developed for the Neutrino Factory and is not yet optimised for a neutrino beam.

Pions are generated and tracked by `MARS` [4].

The advantage of using a magnetic horn is that it is possible to select the focused particle charge, allowing production of a ν_μ, $\overline{\nu}_\mu$ beam by simply reversing the horn current polarity.

A cylindrical decay tunnel has been considered and a systematic study of neutrino fluxes as a function of tunnel length and radius has been performed. It is assumed that the proton beam and the decay tunnel are in line with the detector and the target. As in reference [1] an analytical calculation of the decay probabilities for both pion and subsequent muon decay has been preferred to a Monte Carlo simulation. Fluxes are calculated considering a target-detector distance of 130 km and 10^{23} pot (protons on target) equivalent to the number of protons expected for one year of SPL run.

3 Fluxes calculations

Each pion produced at the target is first propagated and tracked through the horn by `MARS` [4]. In this first step, pions are allowed to decay and the resulting muons are kept, but not the muon neutrinos. The resulting pions and muons at the exit of the horn are then considered. The probability to

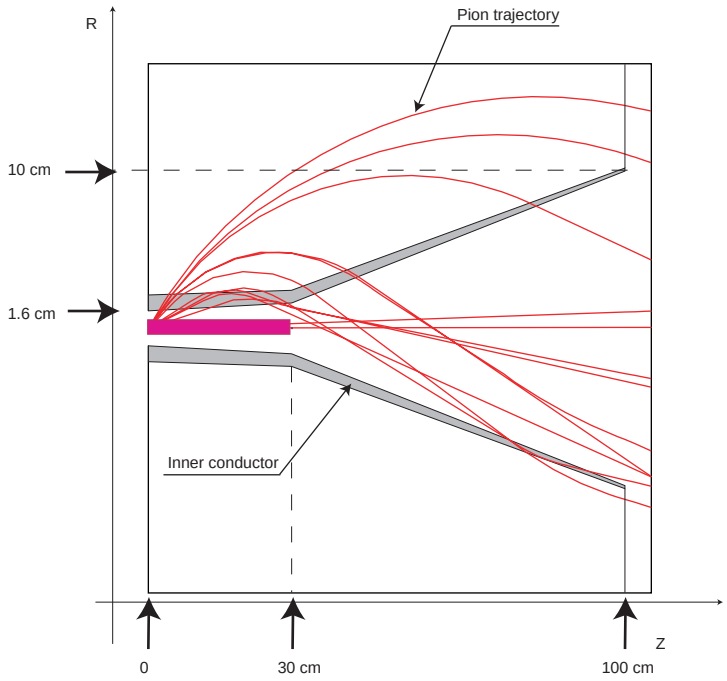

Figure 1: Focusing system

decay within the decay tunnel is calculated and the probability that the resulting neutrino reaches the detector is evaluated.
If a particle reaches the tunnel decay walls, it is assumed to have been absorbed and no further decay is considered. The tunnel radius and length are considered negligible with respect to the target-detector distance.

3.1 Neutrino from pion decay

The probability that a neutrino, coming from pion decay,

$$\pi^{\pm} \rightarrow \mu^{\pm} \, (\overline{\nu}_{\mu})$$

reaches the detector of area A at a distance L is:

$$P\left(\alpha, \beta\right) = \frac{1}{4\pi} \left(\frac{A}{L^2}\right) \frac{1-\beta^2}{(\beta cos\alpha - 1)^2}$$

with
α = angle between pion trajectory and decay tunnel-detector axis;

β = speed of the pion (in units of the speed of light);
A = detector area;
L = distance between decay tunnel and detector.
This formula is valid when the target-detector distance is much larger then the linear dimension of the detector (so that the solid angle covered by the detector can be considered small).
For a complete derivation of this formula we refer to reference [5].

3.2 Neutrinos from muon decay

In the first evaluation of neutrino fluxes from 2.2 GeV protons [1] the muon decay analysis was performed without considering muon polarization.

$$\mu^{\pm} \rightarrow e^{\pm} \nu_e \, (\overline{\nu}_{\mu})$$

In this note the same integration technique is used but the muon decay formula with muon polarization is considered.
The neutrino (antineutrino) helicity has a fixed value of -1 (+1) (neutrino masses are negligible) and the conservation of the angular momentum implies that the positive (negative) muon is completely polarized longitudinally in the pion rest frame with helicity -1 (+1). A Lorentz transformation in the direction of the muon velocity does not change the component of its spin in this direction and so the muon is also completely polarized in its own rest frame. However in the transformation of the muon to the laboratory frame, an angle develops between the transformed muon momentum and spin. As a result the magnitude of the longitudinal polarization, or averaged helicity, in the laboratory frame is generally less than 1 [6]. Figure 2 shows the variation of the averaged muon helicity in the laboratory frame as a function of the pion momentum.

The analytic formula for the probability density that a muon with a certain angle with respect to the target-detector axis and a certain energy produces a ν_e or a ν_μ that reaches the detector is as follows. It is still assumed that the proton beam and the decay tunnel are in line with respect to the target and the detector.

$$\frac{d\mathcal{P}}{dE_\nu} = \frac{1}{4\pi} \frac{A}{L^2} \frac{2}{m_\mu} \frac{1}{\gamma_\mu \left(1 + \beta_\mu \cos\theta^*\right)} \frac{1 - \beta_\mu^2}{\left(\beta_\mu \cos\delta - 1\right)^2} \left[f_0(x) \mp \Pi_\mu f_1(x) \cos\theta^*\right] \tag{1}$$

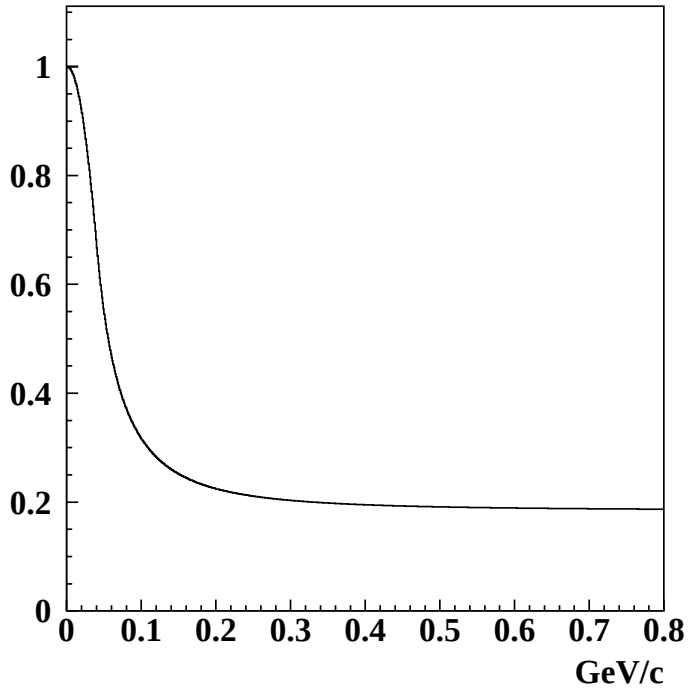

Figure 2: Magnitude of the averaged muon helicity in the laboratory frame

where:
$x = \frac{2E_\nu}{E_\mu} \frac{1}{(1+\beta_\mu \cos\theta^*)}$
E_ν, E_μ = neutrino and muon energy respectively in the laboratory frame;
β_μ, γ_μ = muon relativistic factors;
θ^* = angle between neutrino momentum vector and muon direction (in the muon rest frame);
A = detector area;
L = target-detector distance;
m_μ= muon mass;
δ= angle between muon trajectory and decay tunnel-detector axis;
Π_μ = muon polarization in the muon rest frame along the muon momentum direction;

Functions $f_0(x), f_1(x)$ are given in table (1)
For a complete derivation of this formula we refer to reference [5].

	$f_0(x)$	$f_1(x)$
ν_μ	$2x^2(3-2x)$	$2x^2(1-2x)$
ν_e	$12x^2(1-x)$	$12x^2(1-x)$

Table 1: Flux functions in the muon rest frame

4 Sensitivity of the neutrino fluxes to the decay tunnel dimensions

The ν_μ flux and the ν_e contamination in the ν_μ beam are sensitive to the decay tunnel length and width. As the decay tunnel length increases, the fraction of pions that decay increases quickly, and reaches a plateau when most of the pions have decayed. The ν_e component in the beam comes from muon decay and increases for a much longer time, since the muon decay length is longer. One therefore expects that the length of the decay tunnel can be used to control and vary the fraction of ν_e in the beam. This interesting feature is specific to this beam in which the kaon production is very small. The most important result of this analysis is that ν_e contamination is controllable and reducible at the level of a few per thousand. It is necessary to point out that the optimal configuration for the beam purity will reduce sensibly the total flux. Hence the use of such a beam in an experiment requires to find a compromise between the flux necessary to acquire enough statistics and the background due to the beam contamination.
The length of the decay tunnel must be optimised between the maximum number of pion decay in flight and lowest number of muon decay in flight. It is necessary to observe that the neutrino energy spectrum is a function of the decay tunnel length: with a short decay tunnel only low energy particles will decay while for long decay tunnel also higher energy one will do. By acting on the length of the decay tunnel it is possible to fix the ratio between the pion and muon decays and then the purity of the beam. Figure 3 shows the fluxes of ν_μ, ν_e for decay tunnel of 5, 20, 50 m, with the magnetic horn focusing π^+.

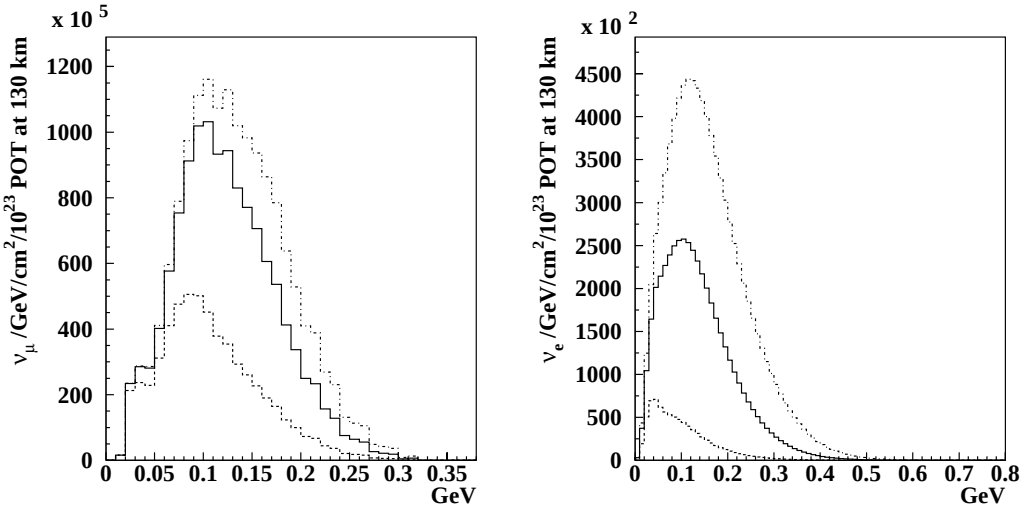

Figure 3: (left) ν_μ, (right) ν_e fluxes for different decay tunnel lengths: (dashed) 5 m, (solid) 20 m, (dotted) 50 m. Fluxes are calculated per GeV, per cm^2 with 10^{23} pot and a target-detector distance of 130 km.

Due to the different pion and muon mean lifetime the ν_e flux still increases when going from 20 m to 50 m decay tunnel length, while the ν_μ flux from pion decays reaches saturation.

A similar study has been performed on the decay tunnel radius but the flux reduction is extremely severe compared with the improvement in beam purity. In Table 2 beam purity, defined as the ratio between the integrated ν_e and ν_μ fluxes, is reported for different combinations of decay tunnel length and radius.
The decay tunnel analysis has been performed with the two polarities of the horn (hence for ν_μ and $\overline{\nu}_\mu$ beams). Results on the $\overline{\nu}_\mu$ beam purity are reported in Table 3.
From this analysis it is possible to imagine the same decay tunnel for both polarities of the horn. It is probably interesting, for the sake of studying systematic errors and flux calibration, to foresee a variable length of the decay tunnel.
For comparison with the previous note [1] we calculated the ratio between the number of ν_e (background) events and $\nu_\mu \to \nu_e$ events (table 4), taking the same assumptions:

Lenght/Radius	25 (cm)	50 (cm)	75 (cm)	100 (cm)
5(m)	0.86	1.12	1.27	1.38
10(m)	1.26	1.76	2.07	2.28
20(m)	1.65	2.53	3.12	3.56
30(m)	1.8	2.98	3.80	4.44
40(m)	1.91	3.27	4.27	5.07
50(m)	1.96	3.45	4.6	5.54

Table 2: Integrated fluxes ν_e/ν_μ, focusing π^+, in fraction per 1000.

Lenght/Radius	0.25 (m)	0.5 (m)	0.75 (m)	1 (m)
5(m)	0.91	1.24	1.45	1.60
10(m)	1.30	1.90	2.27	2.54
20(m)	1.67	2.65	3.32	3.82
30(m)	1.82	3.08	3.98	4.69
40(m)	1.90	3.34	4.43	5.3
50(m)	1.95	3.51	4.74	5.75

Table 3: Integrated fluxes $\bar{\nu}_e/\bar{\nu}_\mu$, focusing π^-, in fraction per 1000.

- horn focusing π^+
- all ν_μ oscillate to ν_e
- ν_e do not oscillate
- neutrino cross section: $0.7\,10^{-38}(cm^2/GeV)$ $\mathrm{E}_\nu(GeV)$.

decay tunnel length	30 m	20 m	10 m	5 m
Ratio without muon polarization	$3.9\ 10^{-3}$	$2.8\ 10^{-3}$	$1.7\ 10^{-3}$	$1.0\ 10^{-3}$
Ratio with muon polarization	$5.0\ 10^{-3}$	$4.0\ 10^{-3}$	$2.2\ 10^{-3}$	$1.3\ 10^{-3}$

Table 4: Ratio between the number of ν_e (background) events and $\nu_\mu \rightarrow \nu_e$ events, considering all ν_μ oscillate to ν_e.

We observed considering muon polarization an increase in the ratio (ν_e/ν_μoscillated) of about 25%.
The final fluxes for a decay tunnel configuration of L=20 m, R=1 m, are shown in Figure 4, 5.

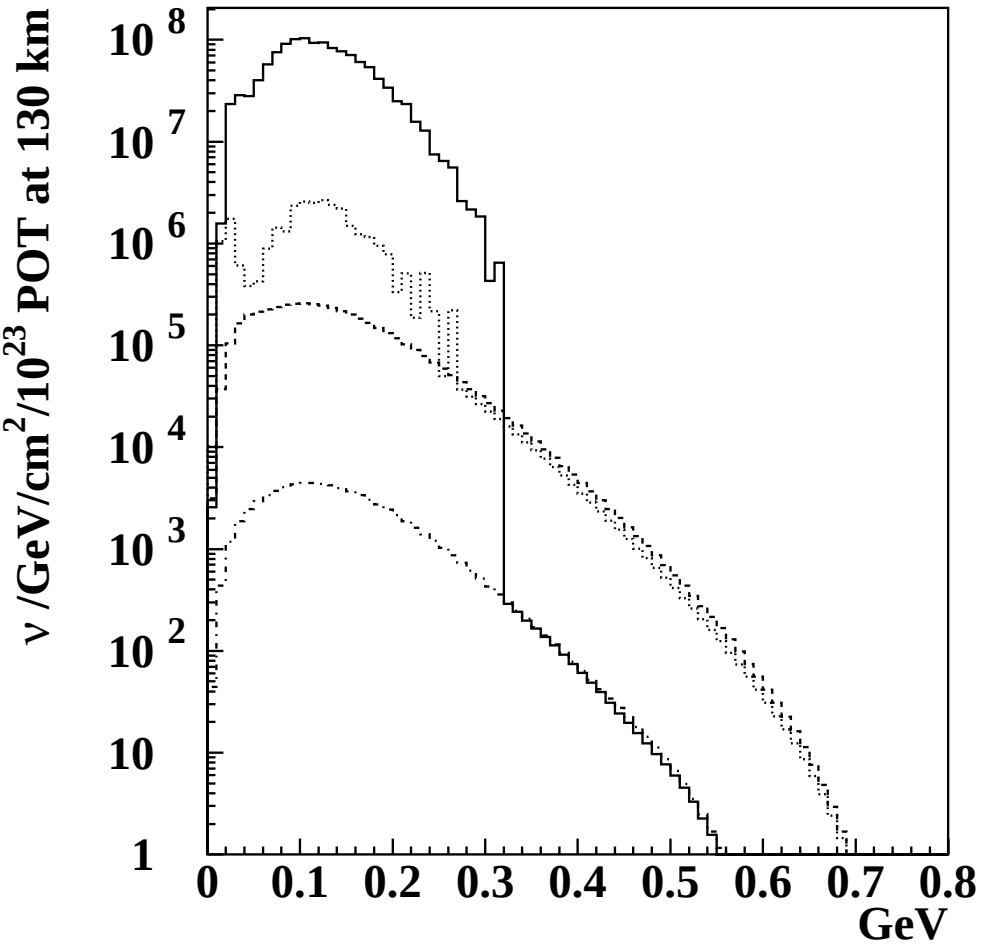

Figure 4: Fluxes obtained with a decay tunnel of 20 m length and 1 m radius focusing π^+: (dotted-dashed) $\overline{\nu}_e$, (dashed) ν_e, (dotted) $\overline{\nu}_\mu$, (solid) ν_μ. Fluxes are calculated per GeV, per cm^2 with 10^{23} pot and a target-detector distance of 130 km.

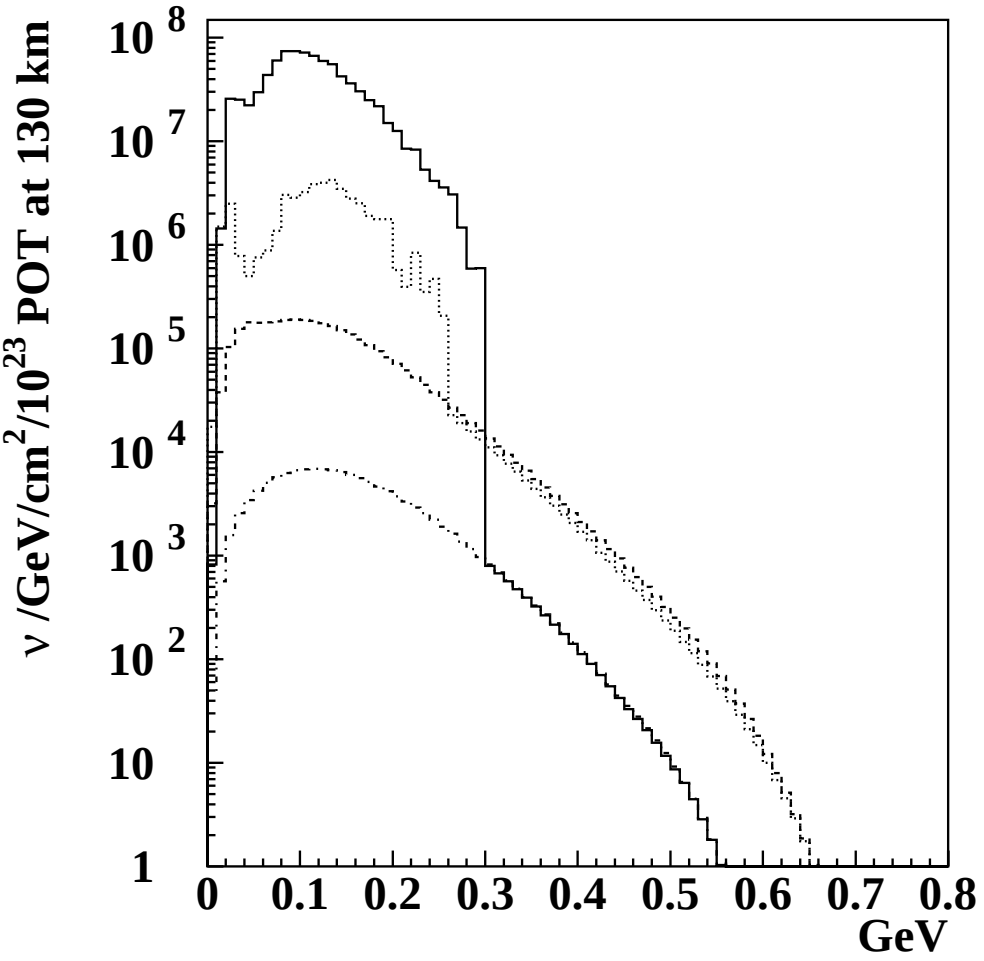

Figure 5: Fluxes obtained with a decay tunnel of 20 m length and 1 m radius focusing π^-: (dotted-dashed) ν_e, (dashed) $\overline{\nu}_e$, (dotted) ν_μ, (solid) $\overline{\nu}_\mu$. Fluxes are calculated per GeV, per cm^2 with 10^{23} pot and a target-detector distance of 130 km.

5 Conclusions

Inclusion of muon polarization effect in the flux calculation is essential, as it increase the ν_e contamination by 25%. The ν_e contamination in the beam is a strong function of the length of the decay tunnel. Given the low energy of the particles in this beam, one can probably foresee a variable length for the decay tunnel, allowing precision systematic error studies. These conclusions are unlikely to be altered in further studies, in which better horn or other focusing device are being developed.

References

[1] A. Blondel *et al.*, "Neutrino Fluxes from a Conventional Neutrino Beam using CERN SPL", NuFact Note 53

[2] A. Ball et al., "Preliminary Magnetic Horn Studies in the Collection Scheme for a Neutrino Factory", proceedings of the NuFact'99 , NIM A 451 (2000) 359-361

[3] A. Ball et al., "Updated results of the horn study for the Nufact", Nufact Note 42

[4] N.V. Mokhov, "The MARS Code System User's Guide", Fermilab-FN-628 (1995)
N.V. Mokhov, "MARS Code Development, Benchmarking and Applications" Fermilab-Conf-00-066(2000)
O.E. Krivosheev and N.V. Mokhov, "A New MARS and its Applications", Fermilab-Conf-98/43 (1998)
N.V. Mokhov, S.I. Striganov, A. Van Ginneken, S.G. Mashnik, A.J. Sierk and J. Ranft, "MARS Code Developments", Fermilab-Conf-98/379 (1998)

[5] M. Donegà, "Study of Neutrino Oscillations with a Low Energy Conventional Neutrino SuperBeam",
available at http://mdonega.home.cern.ch/mdonega/lowe/lenshome.html

[6] F. Combley, E. Picasso, Phys.Rept. **14**, (1974).